

Cosmic Axion Spin Precession Experiment (CASPER)

Dmitry Budker,^{1,2} Peter W. Graham,³ Micah Ledbetter,⁴ Surjeet Rajendran,³ and Alex Sushkov⁵

¹*Department of Physics, University of California, Berkeley, California 94720, USA*

²*Nuclear Science Division, Lawrence Berkeley National Laboratory, Berkeley, California 94720, USA*

³*Stanford Institute for Theoretical Physics, Department of Physics, Stanford University, Stanford, CA 94305*

⁴*AOSense, 767 N. Mary Ave, Sunnyvale, CA, 94085-2909*

⁵*Department of Physics, and Department of Chemistry and Chemical Biology, Harvard University, Cambridge, MA 02138, USA.*

We propose an experiment to search for QCD axion and axion-like-particle (ALP) dark matter. Nuclei that are interacting with the background axion dark matter acquire time-varying CP-odd nuclear moments such as an electric dipole moment. In analogy with nuclear magnetic resonance, these moments cause precession of nuclear spins in a material sample in the presence of a background electric field. This precession can be detected through high-precision magnetometry. With current techniques, this experiment has sensitivity to axion masses $m_a \lesssim 10^{-9}$ eV, corresponding to theoretically well-motivated axion decay constants $f_a \gtrsim 10^{16}$ GeV. With improved magnetometry, this experiment could ultimately cover the entire range of masses $m_a \lesssim \mu\text{eV}$, just beyond the region accessible to current axion searches.

I. INTRODUCTION

The discovery of non-gravitational interactions between dark matter and the standard model can provide insights into particle physics and may allow new probes of the Universe. The Weakly Interacting Massive Particle or WIMP has attracted significant theoretical and experimental attention. While the WIMP is a well motivated candidate, its possible interactions with the standard model are heavily constrained by null results from a variety of experiments [1, 2]. Further, direct probes at the Large Hadron Collider of ideas such as supersymmetry that have provided the theoretical basis for WIMP dark matter have also placed stringent constraints on such scenarios [3]. Indeed, these constraints are most easily alleviated by allowing for a rapid decay of the supersymmetric WIMP candidate (e.g. [4]), precluding a cosmological role for it. Owing to these direct constraints, as well as our ignorance of physics beyond the standard model, it is essential to develop techniques to search for a wide class of dark matter candidates.

Introduced as a solution to the strong CP problem [5, 6], the axion is a prominent dark matter candidate. It arises naturally as the pseudo Goldstone boson of some global symmetry that has a mixed anomaly with QCD and is broken at a high scale f_a [7–12]. QCD generates a potential $\frac{1}{2}m_a^2 a^2$ for the axion with $m_a \sim \frac{\Lambda_{\text{QCD}}^2}{f_a}$. An initial displacement of the axion field from its minimum will result in oscillations of this field with frequency $m_a \frac{c^2}{h}$. The energy density in these oscillations can be dark matter [13, 14]. Other types of light bosons, often called axion-like particles (ALPs), have attracted significant attention [15–27, 56]. These may be pseudo Goldstone bosons of broken symmetries that do not have a mixed anomaly with QCD. They can acquire masses through their coupling with strongly coupled hidden sectors or explicit breaking of the associated global symmetry. While the ALP mass is much less constrained than the axion mass, we focus on light ALPs with masses m_a comparable to that of the axion. Upon acquisition of such a mass, much like the axion, oscillations of the ALP field can also be dark matter. We will use ALP to refer to any of these light bosons, including the QCD axion.

A light particle like an ALP ($m_a \ll \text{meV}$) can be a significant component of dark matter only if it has a large number density, leading to a large field occupation number. The dark matter ALP is a background classical field oscillating at a frequency $m_a \frac{c^2}{h}$ [13, 14] and can be expressed as $a_0 \cos(m_a t)$. The amplitude a_0 is obtained by setting the energy density in the field $\frac{1}{2}m_a^2 a_0^2$ equal to the local dark matter density $\rho_{\text{dm}} \sim 0.3 \frac{\text{GeV}}{\text{cm}^3}$ (see [56] for specific formulae). The temporal coherence of these oscillations in an experiment is limited by motion through the spatial gradients of the ALP field. The gradients are set by the de Broglie wavelength of the ALP $\frac{1}{m_a v}$, where $v \sim 10^{-3}$ is the galactic virial velocity of the axion dark matter. Since the velocity between the experiment and the dark matter is also v , the time τ_a over which the ALP will interact coherently is at least $\tau_a \sim \frac{2\pi}{m_a v^2} \sim 10^6 \frac{2\pi}{m_a}$, or for the axion $\sim 1 \text{ s} \left(\frac{f_a}{10^{16} \text{ GeV}} \right)$. In other words, the ALP's frequency $m_a \frac{c^2}{h}$ is broadened by its kinetic energy $m_a v^2$. Lighter ALPs, corresponding to larger f_a for the QCD axion, are coherent for longer.

The properties of the axion are entirely determined by f_a . Astrophysical bounds rule out axions with $f_a \lesssim 10^{10}$ GeV [28]. When $f_a \gtrsim 10^{12}$ GeV, the oscillations of the cosmic axion can be all of the dark matter [13, 14]. The conversion of axions into photons in the presence of a magnetic field can be used to search for axions with $f_a \sim 10^{12}$ GeV [29, 30]. The ability of such techniques to probe axions with $f_a \gg 10^{12}$ GeV is limited. It is important to develop techniques that can search for axions over the vast majority of its parameter space up to $f_a \sim 10^{19}$ GeV,

especially because of the generic theoretical expectation that the symmetry breaking scale f_a should be close to other fundamental scales in particle physics such as the grand unified ($\sim 10^{16}$ GeV) and Planck scales [31]. While axions with $f_a \gtrsim 10^{12}$ GeV used to be said to be ruled out by cosmological arguments, this bound was based on a simplified picture of cosmology and is not a rigorous bound (see for example [32, 56]).

A technique to search for axions with $f_a \gtrsim 10^{16}$ GeV was suggested in [33]. The key observation of [33] is that the dark matter axion induces a time varying nucleon electric dipole moment (EDM) $d_n \sim 10^{-16} \frac{a_0 \cos(m_a t)}{f_a} e \cdot \text{cm}$. This EDM is generated from the defining coupling $\frac{a}{f_a} \text{tr } G\tilde{G}$ of the axion to QCD [7–12], caused by the same QCD dynamics that leads to physical effects for the operator $\theta_{\text{QCD}} \text{tr } G\tilde{G}$ (e.g. nucleon EDMs $d_n \sim 10^{-16} \theta_{\text{QCD}} e \cdot \text{cm}$) [34], resulting in the strong CP problem and its resolution, the axion. The dark matter axion induces a nucleon EDM of magnitude $10^{-34} e \cdot \text{cm}$ independent of f_a . While this value is much smaller than the current bound on the static nucleon EDM $\sim 10^{-25} e \cdot \text{cm}$, the EDM induced by the dark matter axion oscillates with the axion field at a frequency $m_a \frac{c^2}{\hbar} \sim \text{MHz} \left(\frac{10^{16} \text{ GeV}}{f_a} \right)$.

All EDM experiments to date have searched for static EDMs and have greatly reduced sensitivity to the oscillating nuclear EDM induced by an axion. But in fact, the oscillation of the EDM should, in some ways, make searches easier. Interestingly, even though the axion is generated by physics at high energies ($f_a \gg 10^{11}$ GeV), its ultra-light mass lies at frequencies accessible in the laboratory. A signal that naturally oscillates at a frequency set by fundamental physics, independent of the details of any particular experiment, should ameliorate the systematic errors that often limit the sensitivity of EDM searches.

It was pointed out in [33] that axion dark matter could be detected in future molecular interferometers using the time varying EDM induced by it. In this paper, we argue that such a time varying EDM can be observed through NMR-based experiments using technology that is presently available. We will further exploit the oscillatory nature of the signal by designing a resonant detector that enhances the signal, potentially allowing detection of the QCD axion.

The nucleon EDM naturally induced by an axion is the primary focus of this paper. However, such interactions may also exist for ALPs and the techniques described in this paper will also search for them [56].

II. EXPERIMENTAL CONCEPT

“Solid-state EDM” experiments [36, 38–41] have been proposed as promising ways to search for static EDMs (both of the electron and of nucleons), and an experimental limit on the electron EDM has been set using these methods [46]. We propose an experiment that uses this approach, together with magnetic-resonance techniques, to search for axion or ALP dark matter.

The idea is to polarize the nuclear spins of a sample of material to achieve net magnetization. An external magnetic field (\vec{B}_{ext}) is applied along this magnetization. An electric field (\vec{E}^*) is applied perpendicular to \vec{B}_{ext} , as in Fig. 1. If there is a nucleon EDM, the nuclear spins precess around the electric field. Once they are no longer aligned with external magnetic field then they will precess around both the electric and magnetic fields. Equivalently, the nuclear spins precess around the electric as seen in a rotating frame in which the magnetic field is eliminated. This results (as seen in the lab frame) in a magnetization at an angle to the applied magnetic field, which precesses around this field with Larmor frequency. This transverse magnetization can be measured with a magnetometer such as a superconducting quantum interference device (SQUID) with a pickup loop oriented as shown in Fig. 1. For a static EDM the transverse magnetization will not build up in time since its direction relative to the electric field continually oscillates. Likewise, when the ALP-induced EDM oscillation frequency is different from the Larmor frequency, no measurable transverse magnetization ensues. However, when the two frequencies coincide, there occurs a resonance akin to that in the usual NMR, where the spins precess around a transverse axis rotating at the Larmor frequency [45]. This effect enhances the precessing transverse magnetization that can be detected with the SQUID magnetometer. The magnitude of the external magnetic field (B_{ext}) is swept to search for a resonance. At time $t = 0$ the spins are prepared along \vec{B}_{ext} , then the magnitude of the transverse magnetization is given by

$$M(t) \approx n p \mu E^* \epsilon_S d_n \frac{\sin \left(\left(\frac{2\mu B_{\text{ext}} - m_a c^2}{\hbar} \right) t \right)}{\frac{2\mu B_{\text{ext}} - m_a c^2}{\hbar}} \sin(2\mu B_{\text{ext}} t), \quad (1)$$

where n is the number density of nuclear spins, p is the polarization, μ is the nuclear magnetic dipole moment, and we assume a spin-1/2 nucleus. Here the signal actually arises from the Schiff moment not the EDM and so involves ϵ_S , the Schiff suppression factor [49], times d_n , the magnitude of the ALP-induced nuclear EDM. Thus $\epsilon_S d$ is the effective EDM of the nucleus in the material and $d_n \epsilon_S E^*$ is the energy shift produced. The resonant enhancement occurs when $2\mu B_{\text{ext}} \approx m_a c^2$. We now consider more specific experimental details.

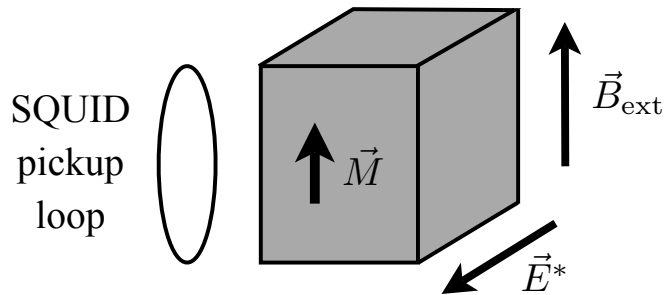


FIG. 1: Geometry of the experiment. The applied magnetic field \vec{B}_{ext} is colinear with the sample magnetization, \vec{M} . The effective electric field in the crystal \vec{E}^* is perpendicular to \vec{B}_{ext} . The SQUID pickup loop is arranged to measure the transverse magnetization of the sample.

The choice of sample material is complicated as there are several tradeoffs. We do not propose a particular material here. Instead we discuss the factors which are involved in this decision and illustrate with examples. The material should be chosen to optimize ϵ_s , p , the transverse relaxation time T_2 , and E^* . Similarly to the situation in WIMP direct detection, many different detector materials may be worth exploring on the path toward detection of axion dark matter.

The sample should be an insulating material containing no unpaired electron spins. The signal is due to the ALP-induced nuclear Schiff moment which scales with $\epsilon_s \propto Z^3$ (Z is atomic number) [47]. So the material should have large- Z atoms whose nuclei have a non-zero magnetic dipole moment, such as ^{207}Pb that has nuclear spin $1/2$. Heavy elements, e.g. Pb or Hg have Schiff suppression factors $\epsilon_s \sim 10^{-2}$. Elements exist with even higher Schiff moments $\epsilon_s \sim 1$, for example the light actinides [43, 44]. These are challenging to work with because they are radioactive.

The nuclear magnetic moments in the sample are polarized by placing it into large magnetic field ($B_0 \approx 10$ T) at low temperature ($\theta_0 \approx 4$ K). A polarization fraction on the order of 10^{-3} can be achieved this way. Higher polarizations may be achievable using optical-pumping techniques. The polarization persists for time, T_1 , set by the spin-lattice relaxation. At cryogenic temperature, T_1 can reach many hours and even longer [42]. It is advantageous to use an element whose nuclear spin is $1/2$, which usually leads to longer spin-lattice relaxation times.

On resonance, the net transverse magnetization precesses at the Larmor frequency ($2\mu B_{\text{ext}}$), as in Eq. (1). The amplitude of the resonant transverse magnetization increases linearly with time, in principle up to the ALP coherence time τ_a . In practice this increase may be cutoff earlier if other effects broaden the resonance. The transverse relaxation time of the nuclear spins, T_2 , may be shorter than τ_a . In this case, T_2 would set the maximum resonant enhancement factor achievable in Eq. (1). In other words if $T_2 < \tau_a$ then the factor $\frac{\sin\left(\left(\frac{2\mu B_{\text{ext}} - m_a c^2}{\hbar}\right)t\right)}{2\mu B_{\text{ext}} - m_a c^2}$ from Eq. (1) would have a maximum $\approx T_2$. The magnetic dipole-dipole interaction between nuclear spins sets the T_2 time to be on the order of 1 ms, however dynamic-decoupling schemes have been shown to increase T_2 substantially [48]. T_2 in excess of 10 s or even 1000 s has been achieved in other materials, see for example, [48, 50, 51].

A material with a crystal structure with broken inversion symmetry at the site of the high- Z atoms is necessary for generation of a large effective electric field E^* , which is proportional to the displacement of the heavy atom from the centro-symmetric position in the unit cell [37]. In a ferroelectric, this displacement can be switched by an external voltage applied to the sample, however, given the oscillating nature of the ALP-induced signal, it may not be necessary to modulate this displacement, in which case any polar crystal can be used. For ferroelectric PbTiO_3 , the effective electric field is $E^* \approx 3 \times 10^8$ V/cm [38]. For other materials, where polarization is permanent, this may be higher by a factor of a few.

Thus, the measurement procedure is as follows. The sample is repolarized after every time interval T_1 . Then the applied magnetic field is set to a fixed value, which must be controlled to a precision equal to the fractional width of the resonance. The magnetic field value determines the ALP frequency (mass) to which the particular shot is sensitive. Then the transverse magnetization is measured as a function of time with fixed applied magnetic field. The total integration time used at any one magnetic field value, t_{shot} , is set by the requirement that an $\mathcal{O}(1)$ range of frequencies can be scanned in 3 years. If T_2 is longer than the ALP coherence time τ_a , then when searching at frequency $m_a \frac{c^2}{\hbar}$ the width of the frequency band is $\approx 10^{-6} m_a \frac{c^2}{\hbar}$. If T_2 is shorter than the ALP coherence time then the width of the frequency band is $\sim \frac{\pi}{T_2}$. Thus we take $t_{\text{shot}} = \frac{10^8 \text{s}}{\min(10^6, \frac{m_a c^2 T_2}{\pi \hbar})}$. Using the magnetization measurements taken over

	n	E^*	p	T_2	Max. B_{ext}
1.	$10^{22} \frac{1}{\text{cm}^3}$	$3 \times 10^8 \frac{\text{V}}{\text{cm}}$	10^{-3}	1 ms	10 T
2.	$10^{22} \frac{1}{\text{cm}^3}$	$3 \times 10^8 \frac{\text{V}}{\text{cm}}$	1	1 s	20 T

TABLE I: Parameters for Phase 1 and 2 regions in Figure 2.

t_{shot} the power in the relevant frequency band around $\frac{2\mu B_{\text{ext}}}{\hbar}$ is found. The applied magnetic field is then changed and the procedure is repeated. The magnetic field should be changed by an $\mathcal{O}(1)$ fraction of the resonance width. After the magnetic field is scanned, the signal of an ALP would be excess power in one band of magnetic fields (ALP frequencies). If multiple ALPs existed they would appear as multiple spikes at different frequencies.

Note that at the lowest frequencies $\lesssim T_2^{-1}$ the resonance is broadened significantly so that an $\mathcal{O}(1)$ range of frequencies is covered in any given frequency bin. An equivalent search in this regime is to use any of the established techniques searching for static nuclear EDMs but with short sampling times $\lesssim \frac{\hbar}{m_a c^2}$, then analyze the data searching for an oscillating signal.

III. SENSITIVITY

The sensitivity of an actual experiment may be limited by the magnetometer, rather than by any of the backgrounds discussed below. We will assume a SQUID magnetometer with a sensitivity of $10^{-16} \frac{\text{T}}{\sqrt{\text{Hz}}}$ as calculated from [35] for a ~ 10 cm diameter sample and pickup loop. This number could possibly be improved with better SQUIDS, a larger sample/pickup loop (see Appendix), or the use of other types of magnetometers. For example, atomic SERF magnetometers could potentially improve on that by another order of magnitude [53, 54].

The magnetometer limit to the sensitivity is determined by the ratio between the signal size in Eq. (1) and the magnetometer sensitivity. The signal will increase linearly in time up to the minimum of T_2 and τ_a . The magnetometer noise goes as $\sim \frac{10^{-16}}{\sqrt{2t}} \frac{\text{T}}{\sqrt{\text{Hz}}}$, so the ratio improves as $\propto t^{\frac{3}{2}}$. Then if T_2 is shorter than τ_a , this ratio will increase $\propto \sqrt{t}$ up to τ_a . From then on it will increase as $t^{\frac{1}{4}}$ (see Appendix this is similar to, for example, [55]). Using the above scalings with integration time t we find the sensitivity curves in Fig. 2.

Figure 2 shows the ALP parameter space that can be explored by searching for time-varying nuclear EDMs. This is a different space than the ALP parameter space that is usually considered, which relies on the ALP coupling to photons. Our sensitivity curves belong in the parameter space of the nuclear EDM coupling. Thus Fig. 2 shows the EDM coupling g_d versus ALP mass. This coupling is defined such that the nucleon EDM is $d_n = g_d a$ where a is the local value of the classical ALP field. The blue and green regions are excluded. The white region is the allowed ALP parameter space. The purple region shows where the QCD axion lies in this parameter space. The dark purple is where the QCD axion may be the dark matter. In order to calculate the limits from previous (static) EDM searches as well as our sensitivity curves, we assume the ALP is all of the dark matter. This parameter space, including the excluded regions and the QCD axion region, is described in detail in [56].

The solid (orange and red) regions in Fig. 2 show estimates for the sensitivity of our proposals. We have made estimates for two phases. Phase 1 (upper, orange region) is a more conservative version relying on demonstrated technology. Phase 2 (lower, red region) relies on technological improvements which have been demonstrated individually but have not been combined in a single experiment of the type we are proposing. Thus the phase 2 proposal may be taken as an estimate of one way to achieve the sensitivity necessary to see the QCD axion with this technique. Since this is a resonant experiment and the frequency must be scanned, realistically it would likely take a few different experiments to cover the entire frequency range in the solid regions. One could choose to spend more time at certain frequencies to improve the limit there, instead of scanning as wide a region.

The dashed (red) line in Fig. 2 shows the ultimate limit on the sensitivity of the phase 2 experiment from sample magnetization noise as in Eq. (A1). This limit could be reached if the magnetometer is improved. The sample magnetization noise limit for the phase 1 experiment is not shown, but was calculated and is not a limiting factor for the phase 1 experiment. Note that this noise is small enough that it would not hinder detection of the QCD axion over the entire relevant frequency range.

For both phases we assumed the nucleus is ^{207}Pb so that $\epsilon_s \approx 10^{-2}$ and the nuclear magnetic moment is $\mu = 0.6\mu_N$, where $\mu_N = 3.15 \times 10^{-14} \frac{\text{MeV}}{\text{T}}$. Other parameters are shown in Table I. With these parameters, the limit on the sensitivity of both phase 1 and phase 2 experiments is set by the magnetometer sensitivity. Improvements in that would lead directly to improvements in the sensitivity of the experiment.

The upper limit on the ALP mass for the solid curves in Fig. 2 comes from requiring that the Larmor frequency be

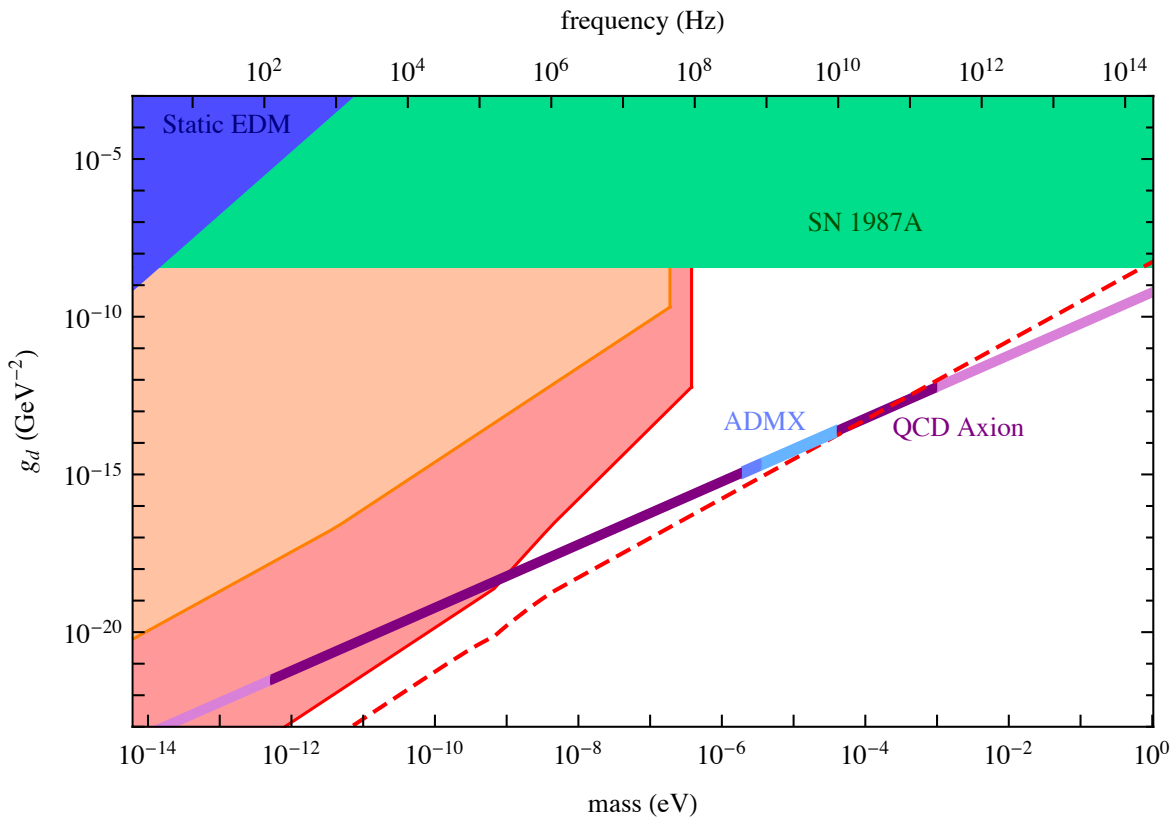


FIG. 2: Estimated constraints in the ALP parameter space in the EDM coupling g_d (where the nucleon EDM is $d_n = g_d a$ and a is the local value of the ALP field) vs. the ALP mass [56]. The green region is excluded by excess cooling of supernova 1987A [56]. The blue region is excluded by existing static nuclear EDM searches [56]. The QCD axion is in the purple region, whose width shows the theoretical uncertainty [56]. The solid red and orange regions show sensitivity estimates for our phase 1 and 2 proposals, set by magnetometer noise. Realistically, it would take several experiments to cover either curve. The red dashed line shows the limit from magnetization noise of the sample for phase 2. The ADMX region shows what region of the QCD axion has been covered (darker blue) [30] or will be covered (lighter blue) [57, 58]. We assume the ALP is all of the dark matter. Current EDM techniques that are optimized to search for a time-varying EDM can already search for ALP dark matter in the allowed region of parameter space [56].

less than the maximum achievable frequency using a 10 T (phase 1) or 20 T (phase 2) applied B-field. The change in slope in the solid phase 2 sensitivity curve comes when the ALP coherence time (τ_a) equals T_2 .

Phase 1 can cover a large piece of unexplored ALP parameter space. Phase 2 reaches the QCD axion for coupling constants $f_a \gtrsim 10^{16}$ GeV. If the magnetometer can be improved and the magnetization noise limit reached, the QCD axion could possibly be detected over the entire region $f_a \gtrsim 3 \times 10^{13}$ GeV.

IV. NOISE SOURCES

Transverse, time varying magnetic fields that overlap with the measurement bandwidth are a source of noise for this experiment. Fluctuations in the transverse magnetization of the sample due to the random flips of the nuclear spins in the sample are a fundamental source of such noise. The quantum projection of each spin along the transverse directions causes an initial transverse magnetization of the sample [39]. The spin projection being random, the net transverse magnetization scales as the square root of the total number of spins. For a sample of size r (and volume $V \propto r^3$), the net magnetic field from this magnetization is $\frac{\mu}{r^3} \sqrt{nr^3} \propto \mu \sqrt{\frac{n}{V}}$. This field precesses at the Larmor frequency $2\mu B$, leading to a power spectrum that is peaked around the Larmor frequency with a bandwidth $\frac{1}{2\pi T_2}$ [39, 52]. This fundamental source of noise can be decreased by using larger sample volumes and is incorporated into the sensitivity plots in Fig. 2. Note that the sensitivity limit set by the magnetization noise (red dashed line) in Fig. 2 would allow detection of the QCD axion over the entire frequency range accessible in this experiment.

An important source of time varying magnetic fields is \vec{B}_{ext} , the magnetic field that is applied to the sample to tune its Larmor frequency close to the ALP's mass. Transverse fluctuations of this field are a source of noise. There are several strategies that can address them. First, field fluctuations caused by the relative mechanical motion of the sample in relation to \vec{B}_{ext} can be minimized by rigidly attaching the sample to the source of the magnetic field. It may also be possible to engineer vibration-isolation systems to damp such sources of noise at the frequencies of interest to this experiment (\gtrsim kHz). Second, superconducting magnets can be used to provide \vec{B}_{ext} , significantly suppressing ac field noise from \vec{B}_{ext} . Third, the phase of the signal depends upon the relative orientation between the nuclear spin (the direction of the EDM) and the internal electric field in the crystal. A differential measurement between two samples where these orientations are different will retain the ALP signal while canceling common-mode magnetic-field noise. With this strategy, it is only the gradients of \vec{B}_{ext} that contribute to the differential signal. These gradients can be minimized through the use of well known coil arrangements such as Maxwell coils. It should be noted that in such coil arrangements, the transverse component of the applied field is also similarly suppressed. Consequently, with this differential-measurement strategy, this noise is suppressed by three potentially small parameters: the initial size of the time variation, the longitudinal gradient, and the size of the transverse component of the applied field.

Certain noise issues can also be addressed by measurements of the malefactor. For example, the longitudinal magnetic field can be measured and used to correct transverse fluctuations if such fluctuations are caused by instabilities in the currents used to provide \vec{B}_{ext} . Similarly, measurements of mechanical motions between the sample and the source of \vec{B}_{ext} can be used to remove the effect of these motions on the magnetic field. Time varying external magnetic fields are also a source of noise and the sample must be screened from them. This can be done using superconducting shields which have been demonstrated to reduce ac field noise by over 10^{13} [59].

Choosing an optimal experimental strategy requires engineering studies that are left for future work. Demanding engineering requirements are encountered in precision magnetometry experiments that can search for static EDMs. For example, the ultimate EDM sensitivity of [51] is comparable to the time varying EDM sought by our experiment. The static EDM searches require control over the dc components of these magnetic fields, while our experiment requires control over the ac component at relatively high frequencies \gtrsim kHz. Such control should be easier to achieve and it thus seems plausible that these sources of noise can be adequately suppressed. For example, control over ac magnetic-field noise at comparable levels in the background of a large external field has been demonstrated in current cavity searches for the axion [30].

V. CONCLUSIONS

The proposed experiment appears to have sufficient sensitivity to detect axion dark matter, especially when f_a is in the theoretically favored range between the grand unified and Planck scales. It is also sensitive to ALPs that couple to the nucleon EDM, making it possible to probe sources of symmetry breaking in the ALP sector. This is the only approach known to us that can be sensitive to this region of parameter space using current technology. Further, in comparison to searches for the dark-matter axion through its couplings to photons, the sensitivity of this approach has only a mild dependence on f_a . This is because the measured spin precession probes the matrix element ($\propto f_a^{-1}$) of the axion interaction. The EDM arises from a non-derivative interaction of the axion and its physical effects are not suppressed by additional powers of the axion wavelength. Indeed, the axion dark matter induced EDM has the same magnitude irrespective of the value of f_a . The dependence on f_a enters through the coherence time τ_a of the axion which limits the resonant build up of the signal. Since $\tau_a \propto f_a$, the sensitivity of this experiment grows with f_a . This is in stark contrast to conventional axion searches that look for axion conversion into photons through the coupling $\frac{a}{f_a} F\tilde{F}$. Such experiments measure cross-sections ($\propto f_a^{-2}$), and for an apparatus of fixed physical size, suffer additional suppressions ($\propto f_a^{-3}$) when the axion wavelengths are longer than this size. This additional suppression occurs because $F\tilde{F}$ by itself is a pure derivative and hence all physical effects of the axion interaction are proportional to derivatives of the axion field.

The EDM oscillates at a frequency set by particle physics, independent of the experimental setup. This distinguishes the signal from many possible backgrounds and should ameliorate the challenges faced by static EDM searches. For example, control over noise sources is only required over the signal's relatively high frequency range (kHz - MHz) and narrow bandwidth ($\sim 10^{-6} m_a \frac{c^2}{\hbar}$). Further, though the induced EDM is small, its oscillation at laboratory frequencies enables resonant schemes that boost the signal significantly. Current EDM techniques that are optimized to search for a time varying EDM can already search for ALP dark matter in the allowed region of parameter space in Fig. 2 [56]. With our resonant scheme, the ultimate sensitivity of this proposal allows for the detection of QCD axion dark matter.

There are several avenues to enhance sensitivity. The signal can be increased using larger sample volumes or with polar crystals that have larger internal electric fields. Other avenues include the use of atomic magnetometers that

can be more sensitive than SQUIDS, as well as the use of dynamic-decoupling techniques that can prolong T_2 . Since the signal scales as the ALP field amplitude $\propto \sqrt{\rho_{\text{dm}}}$, these gains can enable searches for ALPs even if they are a smaller fraction of dark matter.

The dark-matter origin of a signal can be verified in many ways. The signal should change with the relative orientation of the nuclear spin and the electric field; it should be in phase with that from another sample that is placed within the ALP de Broglie wavelength ($\gg 300$ km). The scanning time over any particular frequency band can be relatively short (~ 100 s, see above). Consequently, if there is evidence of a signal at any particular frequency, the apparatus can be tuned to that frequency to determine if the signal builds up in that band as expected. These handles can be used to establish confidence in the detection of a signal.

The experiment we propose may be able to detect ALP and QCD axion dark matter over a wide range of masses. This allows detection of the QCD axion in the high f_a region, where no other current or planned experiment can come close to detecting it. In fact, with improvements in the technology, perhaps with atomic magnetometers, this technique could be used to detect the QCD axion with f_a essentially all the way down to the region that can be probed by microwave cavity experiments such as ADMX. Together then, these techniques may cover almost the entire QCD axion dark matter range.

Similarly to the state of WIMP direct detection at its beginning, there are serious technical challenges that must be overcome for our proposed axion direct detection technique to reach its ultimate sensitivity. But, the case for axion (and ALP) dark matter is strong enough to merit the necessary effort. As with WIMP detectors, this is a scalable experiment with several possible avenues for improvements in sensitivity. A discovery in such an experiment would have profound consequences for physics since it would reveal not just the nature of dark matter and establish the axion as the solution to the strong CP problem, but also provide a window into some of the highest energy scales in nature.

Acknowledgements

We would like to thank Blas Cabrera, Savas Dimopoulos, Matt Pyle, and Scott Thomas for valuable discussions. SR was supported by ERC grant BSMOXFORD no. 228169. This work has been supported in part by the National Science Foundation under grant PHY-1068875. D.B. acknowledges support by the Miller Institute for Basic Research in Science.

Appendix A: Supplemental Materials

1. Magnetization Noise

The intrinsic magnetization noise of the sample is due to the random flips of the nuclear spins. A model for this spin noise was presented in [52], and its power spectrum $S(\omega)$ was found to be

$$S(f) = \frac{1}{8} \left(\frac{T_2}{1 + T_2^2 (2\pi f - 4\pi\mu B)^2} \right). \quad (\text{A1})$$

The spin noise is peaked around the Larmor frequency $2\mu B$ with a bandwidth $\frac{1}{T_2}$. This spectrum was used to estimate the magnetization noise in Fig 2. The model of [52] is an approximation to the noise in a real material. But, the parametric features of this model such as the noise peak at the Larmor frequency with a bandwidth set by T_2 and its dependence on sample volume are expected to be realized in a real material [39].

We integrate this noise over the frequency bandwidth being measured (around any particular axion mass):

$$I = \int_{2\mu_N B + \delta f - \frac{1}{4\pi T_b}}^{2\mu_N B + \delta f + \frac{1}{4\pi T_b}} S(f) df \quad (\text{A2})$$

where $\delta f \sim$ is the offset of the center of the axion signal from the Larmor frequency, and T_b is defined to be the "signal bandwidth time" so that $\frac{1}{2\pi T_b}$ is the bandwidth of the signal region being searched in. T_b is taken to be the smaller of the axion coherence time τ_a and T_2 for the measurement because whichever of these times is smaller defines the bandwidth in which we are looking for the signal. Note of course that T_2 can never physically be longer than the integration time at a particular frequency, though this requirement is not relevant given that the longest T_2 we have chosen to plot in Figure 2 is $T_2 = 1$ s which is always shorter than the integration time at any frequency.

Then the magnetic field noise is

$$B_{\text{noise}} \approx \mu \sqrt{\frac{n}{V}} I \quad (\text{A3})$$

where V is the volume of the sample. We convert this to the limit on g_d exactly as done above for the magnetization signal. In particular, we take the same scalings with time. So the noise improves linearly in time up to the smaller of T_2 and τ_a , then like the square root up to τ_a (if $\tau_a > T_2$), then like the fourth root up to the full integration time at this axion mass.

Note that there are cases where $T_2 > \tau_a$ (at the larger axion masses). We are still allowed to take such a large T_2 even though it is longer than the time of an individual measurement τ_a so long as it is shorter than the full integration time at this particular axion mass. This is because physically one may keep running the experiment and measuring the transverse magnetization of the sample without repolarizing it up to a time T_1 . This helps keep the magnetization noise curve lower at the higher axion masses. This is not necessary for the experiment described here because even if we limited T_2 to be no longer than τ_a the magnetization noise curve would still be below the magnetometer noise curve in Figure 2 (and this of course does not affect the magnetometer noise curves). However, this technique would be useful if for example magnetometers improved and the magnetometer noise was lowered. Then the limit set by the magnetization noise would still allow observation of the QCD axion over the entire accessible region with frequencies $\lesssim 10^8$ Hz.

2. Magnetometer Noise

The transverse magnetization produced by the sample can be measured with a Superconducting Quantum Interference Device (SQUID) magnetometer. The magnetic flux from the sample is collected by a pickup coil (see Fig. 1) that is inductively coupled to a SQUID. The SQUID signal is proportional to the magnetic flux through the SQUID, which can be expressed in terms of sample magnetization M as

$$\Phi_{sq} = 4\pi M \left[gA \frac{NM_{in}}{L_{in} + L_p^{(N)}} \right], \quad (\text{A4})$$

where g is the sample demagnetization factor [60], A is the pickup loop area (matched to sample area), N is the number of pickup loop turns (which is chosen to optimize the coupling to the SQUID), M_{in} is the SQUID-input coil mutual inductance, L_{in} is the SQUID input coil self-inductance, and $L_p^{(N)}$ is the N -turn pickup coil self-inductance, which is roughly proportional to the length of the pickup coil wire. We use the following parameters of a commercially-available SQUID: $M_{in} = 10$ nH, $L_{in} = 1.5$ μ H. If the sample area $A = 80$ cm² (which corresponds to a cylindrically-shaped sample of radius 5 cm), the demagnetization factor $g \approx 0.7$, and the optimal number of pickup loop turns is $N = 2$. These parameters set the value of the expression in the square brackets in Eq. (A4), which we call the ‘‘effective sample area’’ $A_{eff} \approx 0.3$ cm².

The typical white noise level of a commercial SQUID is $\delta\Phi_{sq} \approx 1$ $\mu\Phi_0/\sqrt{\text{Hz}}$. Using the above parameters, we can convert this to an effective magnetic field noise level of $\delta B_{sq} \approx 0.1$ fT/ $\sqrt{\text{Hz}}$, which is the value used in the text.

3. Sensitivity Scaling with Averaging Time

Consider a sinusoidally-varying magnetic field signal with frequency f_0 and amplitude B_0

$$B(t) = B_0 \sin(2\pi f_0 t + \phi(t)) + B_n(t), \quad (\text{A5})$$

where $B_n(t)$ is noise, which we assume to be white, with power spectral density S_n . The signal has a phase coherence time τ ; we model this by assuming that the phase $\phi(t)$ remains constant at short times, and executes random jumps, separated by time τ , to values uniformly distributed within the range 0 to 2π . Ignoring factors of order unity, we derive signal-to-noise scaling with averaging time T , for two cases: 1) $T < \tau$, 2) $T > \tau$.

Consider the function

$$P(f) = \frac{1}{\sqrt{T}} \int_0^T B(t) \sin(2\pi ft) dt = P_0(f) + P_n(f). \quad (\text{A6})$$

This is a Fourier transform, normalized in such a way so as to ensure that the noise energies $|P^2|$ add over consecutive time intervals; P_0 and P_n correspond to the signal and the noise transforms.

In the limit $T \rightarrow \infty$, $|P_n(f)|^2 \rightarrow S_n$ [61]. However, $P_n(f)$ is not a smooth function, each of the independent Fourier components, separated by frequency intervals $1/T$, is randomly distributed according to a Gaussian distribution centered at zero and with variance S_n . From now on we shall focus on the quantity $|P(f)|^2 = |P_0(f)|^2 + |P_n(f)|^2$. Both the expectation value and the standard deviation of $|P_n(f)|^2$ are equal to S_n . Now let us compute $|P_0(f)|^2$.

1) The signal is phase coherent: $T < \tau$. Provided $T \gg 1/f_0$, the Fourier transform vanishes everywhere except at $f = f_0$, where (ignoring factors of order unity) $|P_0(f_0)|^2 = B_0^2 T$. The measurement sensitivity B_s is the value of B_0 that satisfies $|P_0(f_0)|^2 = |P_n(f_0)|^2$, which yields

$$B_s = \sqrt{S_n} T^{-1/2}. \quad (\text{A7})$$

2) The measurement time is longer than signal coherence time: $T > \tau$. The key point is that the signal Fourier transform $|P_0(f)|^2$ is no longer a “delta function”, but now has a linewidth $1/\tau$. The peak amplitude $|P_0(f_0)|^2$ no longer grows with measurement time, but is a constant. We estimate this amplitude by breaking up the time-integral in Eq. (A6) into T/τ pieces of duration τ , and adding them in quadrature, since they have random phase pre-factors. Each piece contributes $B_0^2 \tau^2$, thus the total value of the integral is $|P_0(f_0)|^2 = B_0^2 \tau$.

If we extracted the measurement sensitivity as in case (1), by simply comparing $|P_0(f_0)|^2$ and $|P_n(f_0)|^2$, then we would find that the sensitivity does not improve with measurement time. However, $|P_0(f)|^2$ now has a linewidth $1/\tau$, which means we now have a signal not just at f_0 , but at many frequencies around f_0 , the number of independent frequency points is T/τ . We now compare $|P_0(f)|^2$ and $|P_n(f)|^2$ for each of these frequency points, or fit a lineshape to $|P(f)|^2$, given noise in $|P_n(f)|^2$. As noted above, the scatter of the noise transform points $|P_n(f)|^2$ is S_n , and now we can effectively average T/τ such points near f_0 . Thus the measurement sensitivity B_s is the value of B_0 that satisfies $|P_0(f_0)|^2 = S_n / \sqrt{T/\tau}$, which yields

$$B_s = \sqrt{S_n} (\tau T)^{-1/4}. \quad (\text{A8})$$

We have the usual scaling $B_s \propto T^{-1/2}$ as long as the signal is phase coherent, but beyond the coherence time the sensitivity scales as $T^{-1/4}$.

-
- [1] Z. Ahmed *et al.* [CDMS and EDELWEISS Collaborations], Phys. Rev. D **84**, 011102 (2011) [arXiv:1105.3377 [astro-ph.CO]].
- [2] E. Aprile [XENON100 Collaboration],
- [3] S. Lowette *et al.* [ATLAS and CMS Collaborations], arXiv:1205.4053 [hep-ex].
- [4] P. W. Graham, D. E. Kaplan, S. Rajendran and P. Saraswat, JHEP **1207**, 149 (2012) [arXiv:1204.6038 [hep-ph]].
- [5] R. D. Peccei, H. R. Quinn, Phys. Rev. Lett. **38**, 1440-1443 (1977).
- [6] R. D. Peccei, H. R. Quinn, Phys. Rev. **D16**, 1791-1797 (1977).
- [7] S. Weinberg, Phys. Rev. Lett. **40**, 223-226 (1978).
- [8] F. Wilczek, Phys. Rev. Lett. **40**, 279-282 (1978).
- [9] J. E. Kim, Phys. Rev. Lett. **43**, 103 (1979).
- [10] M. A. Shifman, A. I. Vainshtein, V. I. Zakharov, Nucl. Phys. **B166**, 493 (1980).
- [11] M. Dine, W. Fischler, M. Srednicki, Phys. Lett. **B104**, 199 (1981).
- [12] A. R. Zhitnitsky, Sov. J. Nucl. Phys. **31**, 529-534 (1980).
- [13] J. Preskill, M. B. Wise, F. Wilczek, Phys. Lett. **B120**, 127-132 (1983).
- [14] M. Dine, W. Fischler, Phys. Lett. **B120**, 137-141 (1983).
- [15] J. L. Hewett, H. Weerts, R. Brock, J. N. Butler, B. C. K. Casey, J. Collar, A. de Gouvea and R. Essig *et al.*, “Fundamental Physics at the Intensity Frontier,” arXiv:1205.2671 [hep-ex].
- [16] A. Ringwald, arXiv:1209.2299 [hep-ph].
- [17] A. Ringwald, arXiv:1210.5081 [hep-ph].
- [18] O. K. Baker, M. Betz, F. Caspers, J. Jaeckel, A. Lindner, A. Ringwald, Y. Semertzidis and P. Sikivie *et al.*, Phys. Rev. D **85**, 035018 (2012) [arXiv:1110.2180 [physics.ins-det]].
- [19] P. Arias, J. Jaeckel, J. Redondo and A. Ringwald, Phys. Rev. D **82**, 115018 (2010) [arXiv:1009.4875 [hep-ph]].
- [20] J. Jaeckel and A. Ringwald, Ann. Nucl. Part. Sci. **60**, 405 (2010) [arXiv:1002.0329 [hep-ph]].
- [21] K. Ehret, M. Frede, S. Ghazaryan, M. Hildebrandt, E. -A. Knabbe, D. Kracht, A. Lindner and J. List *et al.*, Phys. Lett. B **689**, 149 (2010) [arXiv:1004.1313 [hep-ex]].
- [22] M. Schott *et al.* [OSQAR Collaboration], arXiv:1110.0774 [hep-ex].
- [23] R. Battesti, M. Fouche, C. Detlefs, T. Roth, P. Berceau, F. Duc, P. Frings and G. L. J. A. Rikken *et al.*, Phys. Rev. Lett. **105**, 250405 (2010) [arXiv:1008.2672 [hep-ex]].
- [24] J. P. Conlon, JHEP **0605**, 078 (2006) [hep-th/0602233].

- [25] A. Arvanitaki, S. Dimopoulos, S. Dubovsky, N. Kaloper and J. March-Russell, Phys. Rev. D **81**, 123530 (2010) [arXiv:0905.4720 [hep-th]].
- [26] B. S. Acharya, K. Bobkov and P. Kumar, JHEP **1011**, 105 (2010) [arXiv:1004.5138 [hep-th]].
- [27] M. Pospelov, S. Pustelny, M. P. Ledbetter, D. F. Jackson Kimball, W. Gawlik and D. Budker, Phys. Rev. Lett. **110**, 021803 (2013) [arXiv:1205.6260 [hep-ph]].
- [28] G. G. Raffelt, Lect. Notes Phys. **741**, 51-71 (2008). [hep-ph/0611350].
- [29] P. Sikivie, Phys. Rev. **D32**, 2988 (1985).
- [30] S. J. Asztalos *et al.* [The ADMX Collaboration], Phys. Rev. Lett. **104**, 041301 (2010) [arXiv:0910.5914 [astro-ph.CO]].
- [31] P. Svrcek, E. Witten, JHEP **0606**, 051 (2006). [hep-th/0605206].
- [32] A. D. Linde, Phys. Lett. B **201**, 437 (1988).
- [33] P. W. Graham and S. Rajendran, Phys. Rev. D **84**, 055013 (2011) [arXiv:1101.2691 [hep-ph]].
- [34] M. Pospelov, A. Ritz, Phys. Rev. Lett. **83**, 2526-2529 (1999). [hep-ph/9904483].
- [35] S. K. Lamoreaux, Phys. Rev. A **66**, 022109 (2002) [nucl-ex/0109014].
- [36] F. L. Shapiro, Sov. Phys. Usp. **11**, 345 (1968).
- [37] S. A. Kuenzi, O. P. Sushkov, V. A. Dzuba and J. M. Cadogan, cond-mat/0205113.
- [38] T. N. Mukhamedjanov and O. P. Sushkov, Phys. Rev. A **72**, 034501 (2005) [physics/0411226 [physics.atom-ph]].
- [39] D. Budker, S. K. Lamoreaux, A. O. Sushkov, and O. P. Sushkov, Phys. Rev. A **73**, 022107 (2006)
- [40] A. O. Sushkov, S. Eckel, and S. K. Lamoreaux, Phys. Rev. A **81**, 022104 (2010).
- [41] K. Z. Rushchanskii *et al.* Nature Mater. **9**, 649 (2010).
- [42] L.-S. Bouchard, A. O. Sushkov, D. Budker, J. J. Ford, and A. S. Lipton, Phys. Rev. A **77**, 022102 (2008)
- [43] N. Auerbach, V. V. Flambaum, V. Spevak, Phys. Rev. Lett. **76**, 4316-4319 (1996). [nucl-th/9601046].
- [44] V. Spevak, N. Auerbach, V. V. Flambaum, Phys. Rev. **C56**, 1357-1369 (1997). [nucl-th/9612044].
- [45] D. Budker, D. Kimball, and D. DeMille (2008) *Atomic Physics: An Exploration Through Problems and Solutions* (New York: Oxford University Press, 2008).
- [46] S. Eckel, A. O. Sushkov, and S. K. Lamoreaux, Phys. Rev. Lett. **109**, 193003 (2012).
- [47] O. P. Sushkov, V. V. Flambaum, and I. B. Khriplovich, Zh. Eksp. Teor. Fiz. **87**, 1521 (1984) [Sov. Phys. JETP **60**, 873 (1984)]
- [48] Y. Dong, R. G. Ramos, D. Li, and S. E. Barrett, Phys. Rev. Lett. **100**, 247601 (2008).
- [49] I. B. Khriplovich and S. K. Lamoreaux (1997), *CP violation without strangeness: Electric dipole moments of particles, atoms, and molecules* Berlin, Germany: Springer (1997)
- [50] M. Ledbetter, S. Pustelny, D. Budker, M. Romalis, J. Blanchard and A. Pines, Phys. Rev. Lett. **108**(24), 243001 (2012) arXiv:1201.4438 [physics.atom-ph].
- [51] M. V. Romalis and M. P. Ledbetter, Phys. Rev. Lett. **87**, 67601 (2001).
- [52] M. Braun and J. Konig, Phys. Rev. B **75**, 085310 (2007)
- [53] H. B. Dang, A. C. Maloof and M. V. Romalis, App. Phys. Lett. **97** (2010) 151110 arXiv:0910.2206 [physics.atom-ph].
- [54] J. C. Allred, R. N. Lyman, T. W. Kornack and M. V. Romalis, Phys. Rev. Lett. **89**, 130801 (2002).
- [55] B. Allen and J. D. Romano, Phys. Rev. D **59**, 102001 (1999) [gr-qc/9710117].
- [56] P. W. Graham and S. Rajendran, New Observables for Direct Detection of Axion Dark Matter, to appear.
- [57] J. Ruz talk at SnowDark 2013. <http://www.physics.utah.edu/snowpac/index.php/snowdark-2013/snowdark-2013-talks-slides>
- [58] ADMX website <http://www.phys.washington.edu/groups/admx/home.html>
- [59] S. Buchman *et al.*, Adv. Space Res. Vol. 25, No. 6, 1177 (2000).
- [60] A. O. Sushkov, S. Eckel, and S. K. Lamoreaux, Phys. Rev. A **79**, 022118 (2009) .
- [61] D. C. Champeney, Fourier Transforms and their Physical Applications, Academic Press (London) 1973.